Carbohydrate Polymers 79 (2010) 775–782

Contents lists available at ScienceDirect

Carbohydrate Polymers

journal homepage: www.elsevier.com/locate/carbpol

A novel strategy to functionalize carbon nanotubes with cellulose acetate using triazines as intermediated functional groups

Gang Ke *

State Key Laboratory of Seismic Reduction/Control and Structural Safety (Cultivation), Guangzhou University, Guangzhou 510006, PR China

ARTICLE INFO

Article history:
Received 21 June 2009
Received in revised form 5 October 2009
Accepted 6 October 2009
Available online 13 October 2009

Keywords:
Carbon nanotubes
Cellulose acetate
Functionalization
Hybrid materials

ABSTRACT

An efficient strategy that consists of cutting, chain extension, introducing active groups and homogeneous reaction tactics was employed to functionalize multiwalled carbon nanotubes (MWNTs) with cellulose acetate (CA). Specially, by utilizing 2,4,6-trichloro-1,3,5-triazine, a novel reactive intermediate of the MWNTs, namely triazine-functionalized MWNTs (MWNT-*triazine*), was obtained. Suitable solubility of the MWNT-*triazine* makes the next homogeneous functionalization of the MWNTs possible. Detailed characterizations further verified that reaction between chloride atoms in the MWNT-*triazine* and hydroxyl groups in the CA had contributed to the formation of MWNT-*CA* conjugates. With a nanotube-attached CA content of 42.8 wt.%, the MWNT-*CA* is readily soluble in intensive polar solvents. Confirmation of the CA-functionalized MWNTs might lead to further studies aiming at potential applications in specific sorption and isolation.

1. Introduction

Covalent functionalization of carbon nanotubes (CNTs) with polymers has been proved to be an effective way to create various hybrid materials with unprecedented properties (Guo, Zhu, Lin, & Zhang, 2008; Yang et al., 2007). To achieve this, it is essential to functionalize the CNTs with ideal polymers. Along with the development of natural polymer science, cellulose and its many derivatives, which combine non-toxicity, biocompatibility, biodegradability and bioactivity with attractive physical and mechanical properties, are becoming increasingly significant (Gandini, 2008). As a distinctive thermoplastic material from nature, cellulose acetate (CA) is one of the most important derivatives of the cellulose, and has broad applications in cigarette filters, separating membranes, optical films, drug delivery systems, antimicrobial agents, food additives, adhesives, textiles, etc. (Kim, Yun, & Ounaies, 2006; Romero, Leite, & Goncalves, 2009). Similarly, owing to unique structures of the nanotubes, the CNTs have shown attractive capabilities in selective adsorption and isolation, as well as drug and other delivery systems (Lu et al., 2009; Yu, Funke, Falconer, & Noble, 2009). Thus, both materials share some important properties. The opportunity to functionalize the CNTs with the CA appears as a desirable way to develop environment-friendly hybrid materials with special properties originated in both components.

As a basis of further studies aiming at potential applications in specific sorption and isolation, e.g. cigarette filter, it is urgent to create functional nanotubes with the CA. Here, we report the first successful covalent functionalization of multiwalled carbon nanotubes (MWNTs) with the CA. Unlike our previous modification of the MWNTs with chitosan (Ke et al., 2007), the CA-based functionalization was accomplished in homogeneous systems.

2. Experimental

2.1. Materials

MWNTs were purchased from Shenzhen Nanotech Port Co. (China). Cellulose acetate with the degree of substitution of 2.2 and the viscometric average molecular weight (M_v) of 1.3×10^5 was obtained from SCRC, China. Other reagents used were of analytical grade.

2.2. Preparation for MWNT-NH_2

After ball-milling, purification and oxidation, MWNTs (4.20 g) in $SOCl_2$ (150 ml) together with *N*,*N*′-dimethylformamide (DMF, 30 ml) were refluxed for 60 h to obtain nanotubes bearing acyl chlorides (Ke et al., 2007). Subsequently, 1,3-propanediamine (1.06 g), triethylamine (10 ml) and acetone (260 ml) were added. The mixture was sonicated for 1 h, then stirred and refluxed under nitrogen for 48 h. After successive procedures of solvent removal, redissolve in acetone, sonication, filtration, water-wash and dryness, MWNTs bearing amino groups were obtained (weight of MWNT-NH_2: 4.20 g).

* Tel.: +86 20 86395053; fax: +86 20 86575840.
E-mail address: kegang@gzhu.edu.cn

0144-8617/$ - see front matter © 2009 Elsevier Ltd. All rights reserved.
doi:10.1016/j.carbpol.2009.10.010

2.3. Preparation for MWNT-triazine

After dissolution of 2,4,6-trichloro-1,3,5-triazine (1.48 g) in THF (120 ml), an ice bath was utilized to maintain temperature of the system below 5 °C. To the mixture, a solution of the MWNT-NH_2 (4.00 g) in THF (100 ml) was added slowly for 8 h with vigorous stirring. The reaction was further carried out over a period of 48 h. Then the mixture was quickly filtered through a 0.22-μm pore size PTFE membrane. The black residue was further extracted with anhydrous acetone in a Soxhlet apparatus at ambient temperature for 48 h, in order to eliminate the excess triazine compound. The final product was dried under vacuum for 24 h (weight of MWNT-*triazine*: 3.64 g; yield: 79.2%).

2.4. Functionalization of the MWNTs with cellulose acetate

A mixture of cellulose acetate (2.26 g), MWNT-*triazine* (0.58 g), acetone (30 ml) and DMF (120 ml) was sonicated for 1 h and vigorously stirred for 1 h. Then the mixture was heated to 40 °C under nitrogen. The reaction was carried out at 40 °C over a period of 6 h. Subsequently, the temperature was raised up to 100 °C and maintained for 48 h. Followed by a complete removal of solvents, the black residue was sonicated in acetone (200 ml) for 30 min, and then filtered through a 0.8-μm pore size nylon filter. After the residue was rinsed with acetone (500 ml), the residue was sonicated in acetone (600 ml) for 30 min and stirred for 2 h. Again the mixture was filtered through nylon membrane. After the rinse-sonication-stir-filtration procedure repeated for another 10 times, the residue was further extracted with acetone in a Soxhlet apparatus at ambient temperature for 72 h, so as to eliminate the excess cellulose acetate. The final product was dried under vacuum for 48 h (weight of MWNT-*CA*: 1.24 g; yield: 43.6%).

2.5. Characterization

FTIR spectra were recorded on a Bruker VERTEX 70 spectrometer from KBr pellets. Solid-state ^{13}C CP/MAS NMR experiments were performed on a Bruker AV400 spectrometer operating at a ^{13}C Larmor frequency of 100.4 MHz. XPS was conducted on a Kratos XSAM 800 spectrometer with a magnesium anode at 400 W, 15 kV and 27 mA (MgKα 1253.6 eV, type 10-360 spherical capacitor analyzer). TEM images were obtained from a FEI Tecnai G2 20 operating at 200 kV. TGA experiments were carried out on a PerkinElmer Pyris *1* TGA system with a typical heating rate of 10 °C min^{-1} in a N_2 atmosphere.

3. Results and discussion

3.1. Synthesis and characterization of triazine-functionalized MWNTs

Our previous functionalization of the MWNTs with chitosan was accomplished by a common approach that based on acylated nanotubes (Ke et al., 2007). However, experiments indicated that the approach was not feasible for the CA-based modification. Firstly, carbon atoms in the acyl chloride groups are just provided by the nanotube sidewalls. As the tube-like structures of graphitic sheets conduce to a higher chemical stability, remarkable steric hindrance and insolubility in any solvent, reactivity of the acylated nanotubes is rather poor. Secondly, cellulose acetate is a polysaccharide derivative that has high molecular weight and stiff molecular chains. This may cause considerable steric hindrance too. Moreover, the reaction was inhomogeneous, which further worsens the functionalization. Thus, as shown in Scheme 1, a strategy that consists of cutting, chain extension, introducing active groups and homogeneous reaction tactics was employed to functionalize the MWNTs with the CA. As displayed in Scheme 1(e), by utilizing 1,3-propanediamine, MWNTs with amino groups extending out from the tube surfaces (MWNT-NH_2) was obtained. Aiming at an efficient graft, it is vital to introduce sufficient and more active groups that can react with hydroxyls of the CA to the nanotube sidewalls. 2,4,6-trichloro-1,3,5-triazine, a basilic compound containing three chlorine atoms with different reactivity, has been widely applied in organic syntheses and polymer modifications (Masllorens, Roglans, Moreno-Mañas, & Parella, 2004; Vollhardt, Liu, & Rudert, 2005; Zhang, Nowlan, Thomson, Lackowski, & Simanek, 2001). Here, the triazine compound was chosen to react homogeneously with the MWNT-NH_2 under low temperature. This could not only double the functional groups of the nanotube

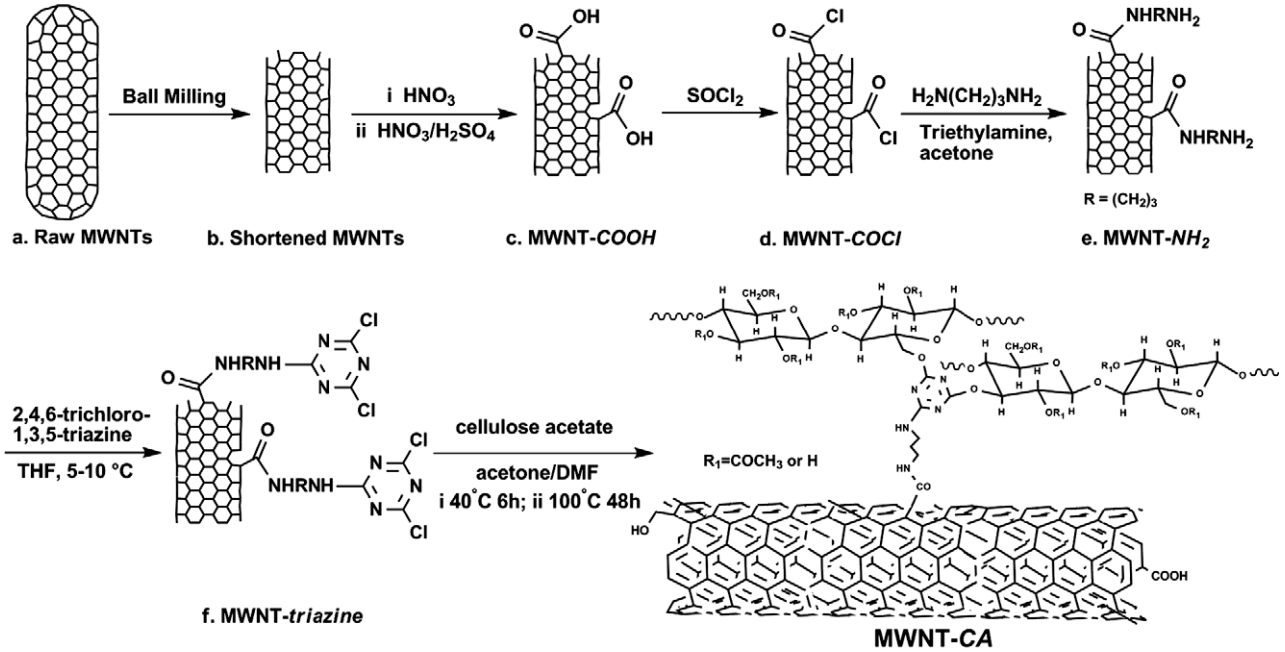

Scheme 1. Functionalization of the MWNTs with cellulose acetate.

sidewalls, but also avoid cross-linking reaction effectively. The obtained novel reactive intermediate, namely triazine-functionalized MWNTs (MWNT-*triazine*, Scheme 1f), was investigated by XPS, FTIR and ^{13}C NMR spectra, as discussed later.

It should be further mentioned that pristine MWNTs are ranging from micrometers to millimeters and highly tangled; tips of the nanotubes are closed, as shown in Fig. 1(a). However, most reactive sites of the nanotubes are their open tips, defects and curves (Chen, Dyer, & Yu, 2001; Liu et al., 1998). By cutting, the long and highly tangled nanotubes may be converted into open tubes-fullerene pips with short lengths; so they can be suspended, sorted and manipulated as individual macromolecules (Liu et al., 1998). For example, shortened MWNTs can be dispersed in polar solvents more easily than crude MWNTs (Saito, Matsushige, & Tanaka, 2002). Therefore, cutting may facilitate reactions of the nanotubes. More importantly, shortened MWNTs are better candidates for adsorbent than pristine MWNTs (Niesz et al., 2002). Aiming at potential applications in specific sorption and isolation, the MWNTs were cut by ball-milling (Fig. 1b and c), and then functionalized with the CA.

FTIR spectra of the MWNT-*COOH*, MWNT-NH_2 and MWNT-*triazine* are shown in Fig.2. After cutting, purification and oxidization, absorptions of O—H, C=O and C—O appear in Fig. 2(a), which indicates the existence of carboxyl groups on the nanotube surfaces. As for Fig. 2(b), characteristic bands of amide occur at 1656, 1548 and 1274 cm^{-1}, corresponding to amide I, II and III, respectively. Moreover, vibration absorptions of C—N and N—H can be observed severally at 1362 and 1176 cm^{-1}. These suggest the nucleophilic substitution reaction between 1,3-propanediamine and acylated nanotubes.

As shown in Fig. 2(c), characteristic absorptions relating to triazine ring occur at 1557, 847 and 790 cm^{-1}, respectively. The 1557 cm^{-1} band is attributable to stretching of C=N in triazine rings (Khabashesku, Zimmerman, & Margrave, 2000); the 847 cm^{-1} band arises from skeleton vibration of the triazine ring; and the 790 cm^{-1} absorption is due to C—Cl vibration. Additionally, the amide III of the MWNT-NH_2 at 1274 cm^{-1} shifted to 1236 cm^{-1} and much enhanced. It may attribute to vibration absorption of C—N in —H*N*—C$NC_2N_2Cl_2$. These changes suggest the substitution reaction between 2,4,6-trichloro-1,3,5-triazine and the MWNT-NH_2.

^{13}C NMR spectra of the 2,4,6-trichloro-1,3,5-triazine, MWNT-NH_2 and MWNT-*triazine* are displayed in Fig.3. The 2,4,6-trichloro-1,3,5-triazine shows symmetrical ^{13}C resonances with low-intensity at 182.7 and 176.8 ppm. This is similar to reports of Jürgens et al. (2003) and Gillan (2000). As for the MWNT-NH_2, broad resonances with high-intensity appear in the range of 14–72 ppm. The consecutive signal peaks at 35.6, 49.8 and 58.4 ppm may be attributed to methylene carbon in —CONH—$CH_2CH_2CH_2$—NH_2. The distinct signal broadening arises from delocalized electrons (a π-electron ring current) in nanotubes (Peng, Alemany, Margrave, & Khabashesku, 2003). In addition, Fig. 3(b) exhibits a characteristic ^{13}C nanotube resonance at 132.8 ppm (Peng et al., 2003) and a ^{13}C signal of amide at 163.9 ppm, respectively.

After the reaction with 2,4,6-trichloro-1,3,5-triazine, ^{13}C NMR spectrum of the MWNT-NH_2 changes obviously. In Fig. 3(c), ^{13}C signals of triazine appear at 180.3, 175.4 and 170.8 ppm, respectively. Each molecule of the 2,4,6-trichloro-1,3,5-triazine contains three chlorine atoms with different reactivity. Under a temperature lower than 10 °C, once any chlorine atom of the triazine ring reacted with amino groups of the MWNT-NH_2, reactivity of the other two chlorine atoms would be suppressed (Xing, Xu, Zhou, & Pei, 2000). Therefore, carbon atoms in the triazine rings were in two kinds of chemical environment after the reaction. Resonance signals of the carbon atoms that still bond with chlorine atoms occur at downfield (180.3 and 175.4 ppm). To the contrary, while nitrogen has a much lower electron-withdrawing ability than chloride, resonance of the carbon atom that bonds with nitrogen atom (—H*N*—C$NC_2N_2Cl_2$) appear at upfield (170.8 ppm). Compared with Fig. 3(b), resonances relating to methylene carbon were further broadened with a range of 5–73 ppm in Fig. 3(c); and shifts of the signal peaks occurred. The changes may arise from the introducing of chloric triazine rings, which have aromatic character and electron-withdrawing ability. ^{13}C NMR results above are consistent with the analysis of FTIR.

To confirm the findings from the IR and ^{13}C NMR spectra, XPS analysis was employed. In Fig. 4(a), XPS survey spectrum of the MWNT-NH_2 presents all expected elements with the content of 89.0 at.% (carbon), 6.4 at.% (oxygen) and 4.6 at.% (nitrogen). Besides carbon, oxygen and nitrogen, the MWNT-*triazine* contains 3.2 at.% of chlorine (Fig. 4b), which should arise from chlorine atoms in the triazine rings.

XPS C 1s spectra of the MWNT-NH_2 and MWNT-*triazine* are illustrated in Fig. 4(c and d). Both materials exhibit the C 1s core levels with similar binding energies, whereas the full-width at half-maximum (FWHM) of the latter is higher than the former by 0.08 eV. It indicates a more complicated bonding environment in the MWNT-*triazine* (Baker, Cai, Lasseter, Weidkamp, & Hamers, 2002; Wada, Murata, Tokunaga, & Watanabe, 2003; Zhang & Wang, 1995). C 1s spectrum of the MWNT-NH_2 has been fitted to three symmetrical components at 284.7, 285.8 and 287.6 eV. As for alkane and graphite-like carbon atoms of the tube-walls, binding energies of *C*—*C* are common of 285.0

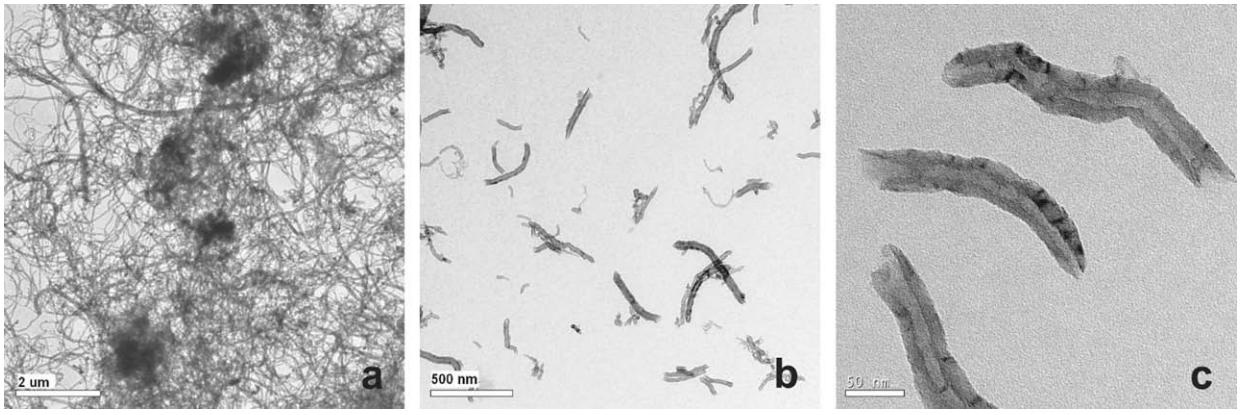

Fig. 1. TEM images of (a) raw MWNTs, (b and c) shortened, purified and acid oxidized MWNTs.

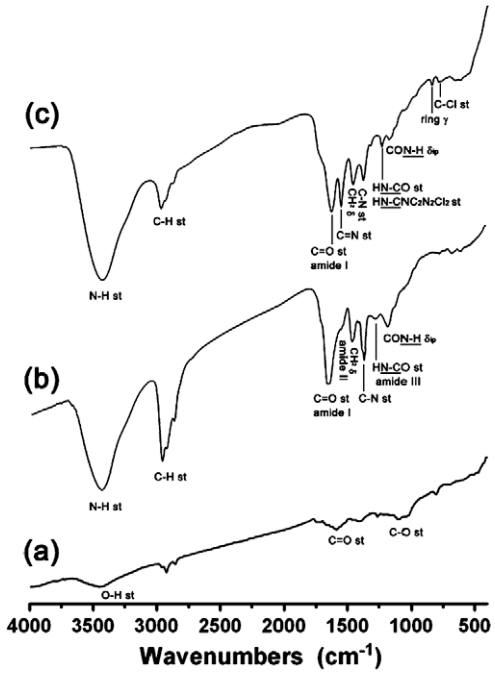

Fig. 2. FTIR spectra of (a) MWNT-*COOH*, (b) MWNT-NH_2 and (c) MWNT-*triazine*.

and 284.4 eV, respectively (Baker et al., 2002; Ramanathan, Fisher, Ruoff, & Brinson, 2005). So the peak at 284.7 eV may be attributed to the nanotubes and alkyl of 1,3-propanediamine. Similarly, the peak at 285.8 eV arises from *C*—N of the propanediamine moieties and *C*—OH that was produced in the purification and oxidation of the MWNTs (Wagner et al., 2007). In addition, the broad signal at 287.6 eV is characteristic emission from amide carbon. It indicates the formation of amide bonds between MWNTs and 1,3-propanediamine. Unlike the MWNT-NH_2, C 1s spectrum of the MWNT-*triazine* has been fitted to four symmetrical components. The additional higher C 1s binding energy of 288.7 eV is characteristic emission from triazine carbon atoms that bonds with chlorine atoms. This indicates the existence of reactive sites in the MWNT-*triazine*.

XPS N 1s spectra of the MWNT-NH_2 and MWNT-*triazine* are illustrated in Fig. 4(e and f). The FWHM of the N 1s core level of the latter is higher than that of the former by 0.42 eV, implying a more complicated bonding environment in the MWNT-*triazine*. In Fig. 4(e), N 1s spectrum of the MWNT-NH_2 shows two components corresponding to amino nitrogen and amide nitrogen at 398.8 and 400.1 eV, respectively (Wagner et al., 2007). This further confirms the existence of amide and amino groups. In Fig. 4(f), N 1s spectrum of the MWNT-*triazine* exhibits two components at 399.1 and 400.2 eV, respectively. The peak at 399.1 eV is characteristic emission from *N*=C in triazine rings (Martins, Wang, Ji, Feng, & Barbosa, 2003; Salmain, Fischer-Durand, Roche, & Pradier, 2006). Owing to the introducing of triazine rings, two kinds of —*NH*— occur in the MWNT-*triazine*: —CO*NH*$(CH_2)_3$— and —$(CH_2)_3$*NH*$C_3N_3Cl_2$. Both tube-linked carbonyl and chloric triazine ring have electron-withdrawing abilities. Hence both kinds of —*NH*— are in similar chemical environments and contributing to the binding energy of 400.2 eV.

Comprehensive analyses above have confirmed chemical structures of the MWNT-NH_2 (MWNT-*CONH*$(CH_2)_3NH_2$), and the MWNT-*triazine* (MWNT-*CONH*—$(CH_2)_3NHC$=$NC_2N_2Cl_2$), as presented in Scheme 1. Furthermore, by TG determinations, content of amino groups in the MWNT-NH_2, and content of triazine rings in the MWNT-*triazine* are estimated to be ca. 1.0 and 0.8 mmol/g, respectively.

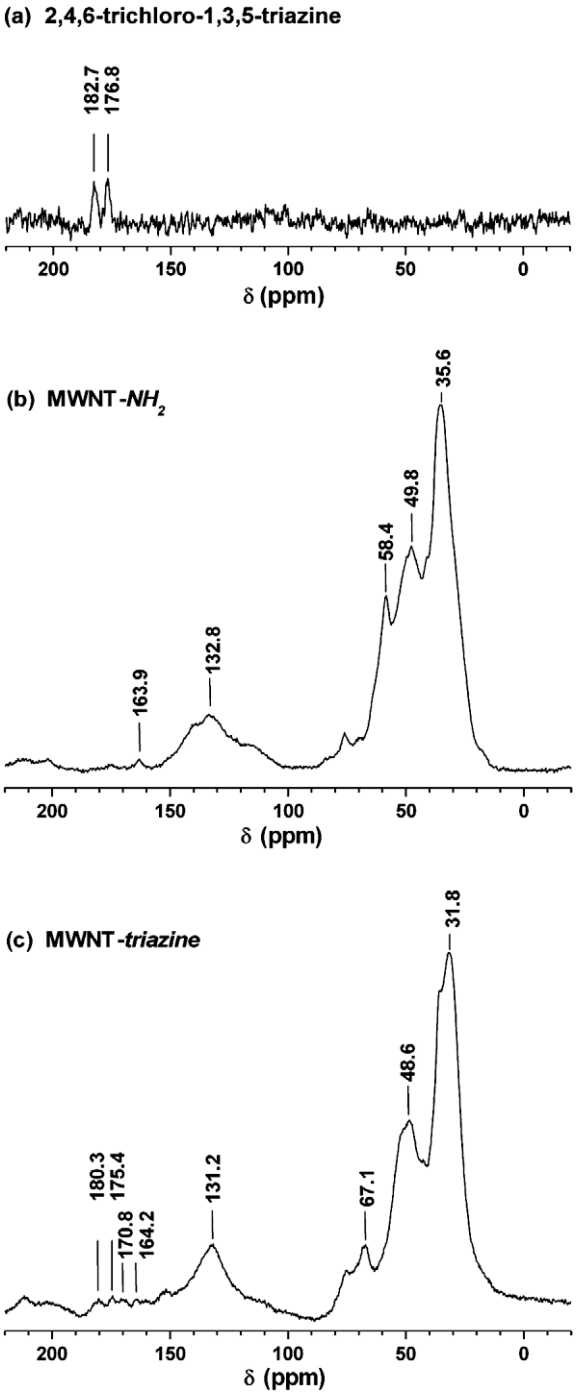

Fig. 3. ^{13}C NMR spectra of (a) 2,4,6-trichloro-1,3,5-triazine, (b) MWNT-NH_2 and (c) MWNT-*triazine*.

3.2. Synthesis and characterization of cellulose acetate-functionalized MWNTs

Unlike the MWNT-NH_2, the MWNT-*triazine* is insoluble in acetone, tetrahydrofuran and dichloromethane, whereas it is easily soluble in pure water and low alcohols. In addition, similar to the MWNT-NH_2, the MWNT-*triazine* dissolves in DMSO, DMF and DMAc, which helps make the functionalization of the MWNTs with CA via homogeneous reaction become reality. Based on following considerations, a mixture of DMF/acetone with a volume ratio of 4:1 was chosen as the medium. (i) The reaction comprises a lower

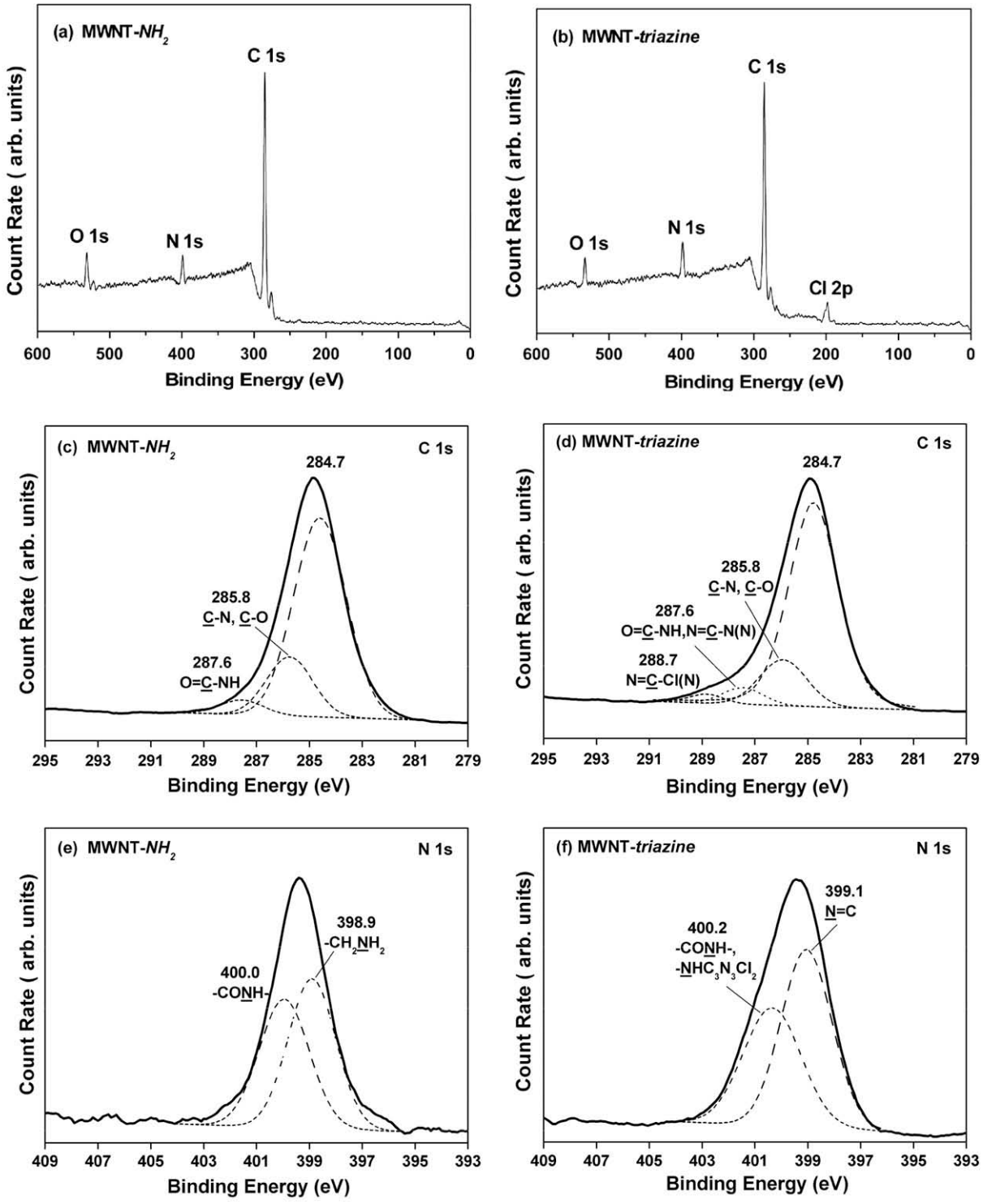

Fig. 4. XPS characterization on the MWNT-NH_2 and MWNT-*triazine*.

temperature stage (40 °C) and a higher temperature stage (100 °C). With a boiling temperature of 153–154 °C, DMF matches this need. (ii) As a common alkaline solvent in the nucleophilic substitution reactions, DMF avails to absorb chlorine hydride released in attacks of the CA molecules on the MWNT-*triazine*. (iii) Although the CA is soluble in DMF, it has a better solubility in acetone.

After the functionalization and separations, a black product was obtained. By TEM imaging, as shown in Fig. 5(a and b), it depicts representative features showing the shortened nanotubes compactly coated with an amorphous polymeric material. Further by magnification, as shown in Fig. 5(c), the nanotubes exhibit their peculiar lattice fringe characteristics, which are completely different from the coated material. That is, the nanotubes and the coating are distinct materials. On one hand, as the product was carefully separated by sonication, rinse and repeated extraction with acetone, any soluble CA should be removed previously. Here, the amorphous material should not be un-reacted or unbounded CA, otherwise it would spread all over the carbon diaphragm and not

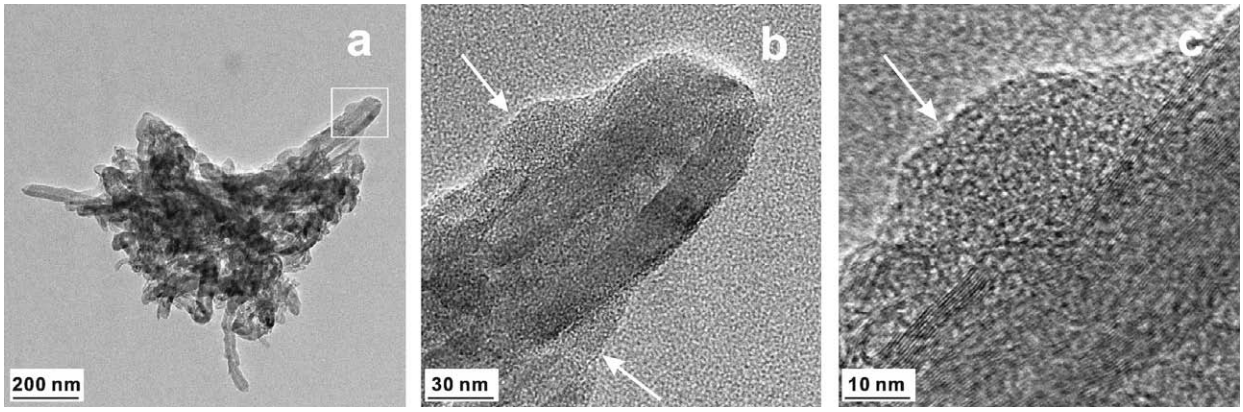

Fig. 5. TEM images of the MWNT-*CA* (White arrows indicate the typical features of attached CA).

localize just on the nanotubes. On the other hand, there is not any detectable clearance between the material and nanotube surfaces. Such a tight conglutination of two distinct materials should not be a result from physical adsorption. Take all these into account, the material surrounding the nanotubes was deduced to be covalently attached CA moieties. Consequently, the purified single resultant, which was considered as the cellulose acetate-functionalized MWNTs (MWNT-*CA*), was worthy of detailed investigation and confirmation.

In FTIR spectrum of the MWNT-*CA* (Fig. 6a), five characteristic bands of the CA appear at 602, 886, 1050, 1159 and 1732 cm^{-1}, respectively. Moreover, C—Cl stretching of the MWNT-*triazine* at 791 cm^{-1} was absent after functionalization. Additionally, vibration absorption of triazine ring skeleton at 1557 cm^{-1} shifted to 1544 cm^{-1} and much weakened after modification. These changes suggest that chlorine atoms in the MWNT-*triazine* have been substituted. It conduced to a linkage formation between the triazine rings and large molecular chains of the CA, which weakened the absorption of ring skeleton (Ning, 2000).

^{13}C NMR spectrum with characteristic carbon resonances of the CA is displayed in Fig. 6(b). Owing to partial esterification of hydroxyls at ortho-C(2), signal of bridge carbon atoms in the glucopyranose rings split, as marked with *C* 1 and *C* 1′. By comparing signal integrated area of the *C* 1 with that of the *C* 1′, degree of substitution at C(2) is ca. 0.18. In ^{13}C NMR spectrum of the MWNT-*CA*, identified resonances originating from the CA can be also observed. The distinct signal broadening is consistent with previous experimental and theoretical studies on functionalized nanotubes (Cahill et al., 2004; Holzinger et al., 2003). These again support the attachment of the CA moieties.

It is surprising that signal of the *C* 1 of the CA is single; however, it split in spectrum of the MWNT-*CA*. Since ^{13}C resonance of the MWNT-*triazine* is very weak in the range of 90–110 ppm (Fig. 3c), signals at 107.4 and 110.7 ppm may be assigned to the bridge carbon in glucopyranose rings of the MWNT-*CA*. Although there are many precedents for complicated split of signals in solid-state ^{13}C NMR spectra of functionalized nanotubes (Cahill et al., 2004; Holzinger et al., 2003), here, signal that is attributed to methyl carbon with the most highest relative intensity, as well as signal that arises from carbonyl carbon do not spilt. So the signal split of the *C* 1 has little relation with the nanotubes. Considering that ^{13}C resonance of the bridge carbon is much affected by

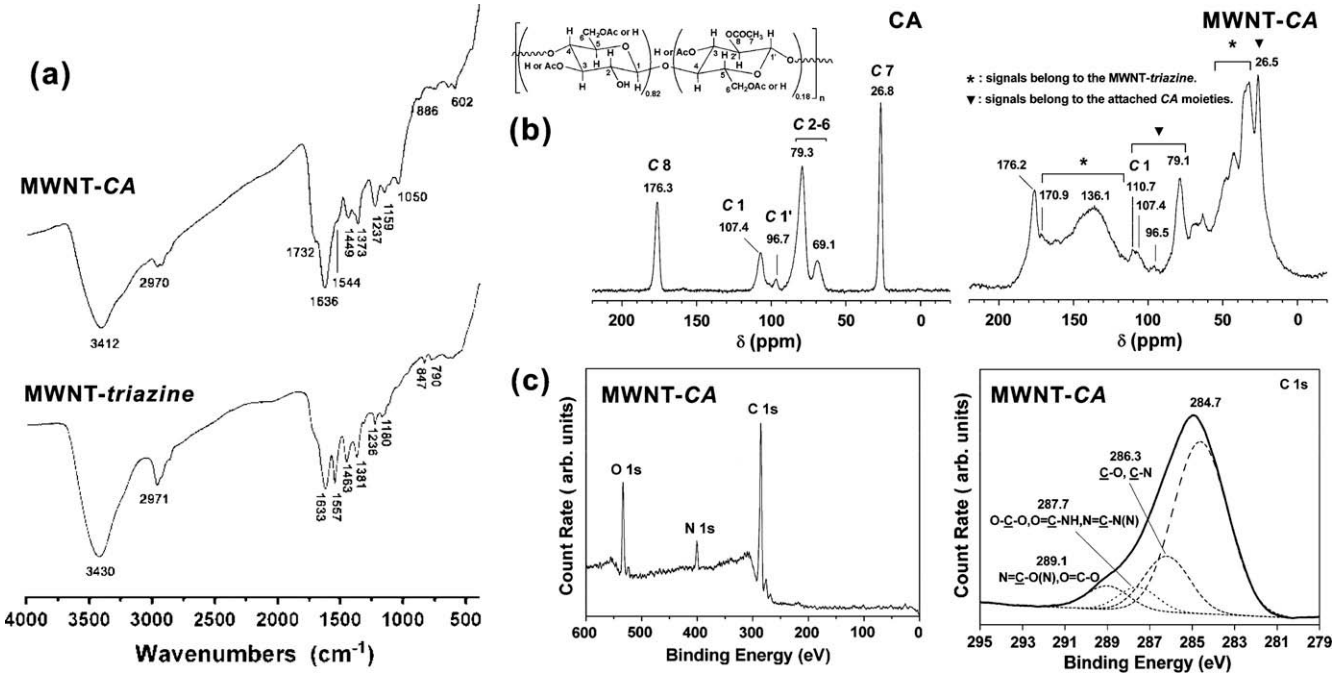

Fig. 6. (a) FTIR spectra of the MWNT-*triazine* and MWNT-*CA*; (b) ^{13}C NMR spectra of the CA and MWNT-*CA*; (c) XPS survey and C 1s spectra of the MWNT-*CA*.

functional groups at ortho-C(2), and the IR results have suggested the occurrence of the reaction, it is possible that a portion of hydroxyls at C(2) reacted with chlorine atoms in the MWNT-*triazine*, as illustrated in Scheme 1. Hence new ether linkages involving carbon in the triazine rings might be introduced to C(2). While the excursion of σ electrons varied the chemical environment of ortho-C(1) (Ning, 2000), the ^{13}C resonance signal split thereof.

To confirm the findings from the IR and ^{13}C NMR spectra, XPS analysis was employed. In Fig. 6(c), XPS survey spectrum of the MWNT-*CA* presents all expected elements with the content of 76.3 at.% (carbon), 18.4 at.% (oxygen) and 5.3 at.% (nitrogen). The absence of chlorine is in agreement with the IR analysis, and further supports the reaction involving chlorine atoms in the triazine rings. As a result of attachment of the CA moieties, a remarkable increase in oxygen content occurred.

XPS C 1s spectrum of the MWNT-*CA* is also illustrated in Fig. 6(c). The FWHM of the C 1s core level of the MWNT-*CA* is larger than that of the MWNT-*triazine* by 1.20 eV. It indicates a more complicated bonding environment in the MWNT-*CA* (Baker et al., 2002; Wada et al., 2003; Zhang & Wang, 1995). After functionalization, the characteristic C 1s peak of the MWNT-*triazine* at 288.7 eV in Fig. 4(d), which arose from the triazine carbon bonded to chloride, was superseded by a new signal with binding energy higher than 289.0 eV. On one side, once the MWNT-*triazine* reacted with the CA, chloride in N═*C*—*Cl*(N) would be replaced by oxygen. Hence a new bond structure of N═*C*—*O*(N) formed. While oxygen has a better electron-withdrawing ability than chloride, it leads to a decrease in out-shell electron density of carbon bound to oxygen. Thus, the shielding effect weakened, the C 1s binding energy increased. On the other side, molecular chains of the CA comprise acetic ester, whereas the C 1s binding energy of ester carbon (CH_3*C*OO—) is about 289.0 eV (Wagner et al., 2007). Similarly, C 1s peak at 285.8 eV that represents the *C*—N and *C*—O contributions, shifted to a higher binding energy of 286.3 eV. It should be related to the bond structures of *C*—O—*C* and *C*—OH in the CA chains (Wagner et al., 2007). In addition, the slightly shifting of C 1s peak at 287.6 eV with an increase in area may arise from the bridge carbon (O—*C*—O) in glucopyranose rings. These XPS findings further approve the attachment of CA to the nanotubes, which is due to the reaction between triazine chloride atoms in the MWNT-*triazine* and hydroxyl groups in the CA.

TG thermograms of the CA, MWNT-*triazine* and MWNT-*CA* samples are shown in Fig. 7. The MWNT-*CA* shows a main and gradual thermal degradation step in the temperature range of 270–600 °C. The onset decomposition temperature and the temperature at the maximum weight loss of the MWNT-*CA* are 270 °C and 358 °C, respectively. At 700 °C, weight of the MWNT-*CA* is 34.9 wt.%. Residuary weight of the CA at 700 °C is 5.9 wt.%, which arises from charring residuals of the cellulose. Based on the TG data, weight content of the attached CA in the MWNT-*CA* was estimated to be ca. 42.8 wt.%.

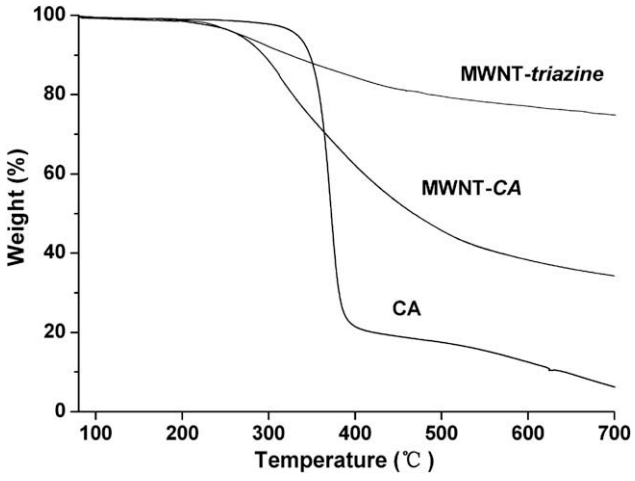

Fig. 7. TG thermograms of the CA, MWNT-*triazine* and MWNT-*CA*.

With aid of the attached CA moieties, the MWNT-*CA* is readily soluble in DMF, DMAc, NMP and DMSO, which makes it possible to mix the MWNT-*CA* together with certain cellulose matrices in homogeneous systems in next application step.

4. Conclusions

In summary, we have demonstrated a novel strategy to functionalize the MWNTs with the cellulose acetate using triazines as intermediated functional groups. Detailed characterizations verified that reaction between chloride atoms in the triazine-functionalized MWNTs (MWNT-*triazine*) and hydroxyl groups in the CA had contributed to the formation of MWNT-CA conjugates. With a nanotube-attached CA content of 42.8 wt.%, the MWNT-*CA* is readily soluble in intensive polar solvents. Confirmation of the CA-functionalized MWNTs might lead to further studies aiming at potential applications in specific sorption and isolation, for example, excellent cigarette filter (Ke, Huan, Huang, Liu, & Liu, 2008).

References

Baker, S. E., Cai, W., Lasseter, T. L., Weidkamp, K. P., & Hamers, R. J. (2002). Covalently bonded adducts of deoxyribonucleic acid (DNA) oligonucleotides with single-wall carbon nanotubes: Synthesis and hybridization. *Nano Letters, 2*, 1414–1415.

Cahill, L. S., Yao, Z., Adronov, A., Penner, J., Moonoosawmy, K. R., Kruse, P., et al. (2004). Polymer-functionalized carbon nanotubes investigated by solid-state nuclear magnetic resonance and scanning tunneling microscopy. *Journal of Physical Chemistry B, 108*, 11412–11418.

Chen, J., Dyer, M. J., & Yu, M. F. (2001). Cyclodextrin-mediated soft cutting of single-walled carbon nanotubes. *Journal of the American Chemical Society, 123*, 6201–6202.

Gandini, A. (2008). Polymers from renewable resources: A challenge for the future of macromolecular materials. *Macromolecules, 41*, 9491–9504.

Gillan, E. G. (2000). Synthesis of nitrogen-rich carbon nitride networks from an energetic molecular azide precursor. *Chemistry of Materials, 12*, 3906–3912.

Guo, H. F., Zhu, H., Lin, H. Y., & Zhang, J. Q. (2008). Synthesis of polyaniline/multi-walled carbon nanotube nanocomposites in water/oil microemulsion. *Materials Letters, 62*, 3919–3921.

Holzinger, M., Abraham, J., Whelan, P., Graupner, R., Ley, L., Hennrich, F., et al. (2003). Functionalization of single-walled carbon nanotubes with (R-)oxycarbonyl nitrenes. *Journal of the American Chemical Society, 125*, 8566–8580.

Jürgens, B., Irran, E., Senker, J., Kroll, P., Müller, H., & Schnick, W. (2003). Melem (2,5,8-triamino-tri-*s*-triazine), an important intermediate during condensation of melamine rings to graphitic carbon nitride: Synthesis, structure determination by X-ray powder diffractometry, solid-state NMR, and theoretical studies. *Journal of the American Chemical Society, 125*, 10288–10300.

Ke, G., Huan, S., Huang, F., Liu, X. G., & Liu, Z. L. (2008). *Cellulose diacetate-carbon nanotube derivative, and its preparation method and application*. CN Patent Office, Pat. Appl. No. 101 239 715.

Ke, G., Guan, W. C., Tang, C. Y., Guan, W. J., Zeng, D. L., & Deng, F. (2007). Covalent functionalization of multiwalled carbon nanotubes with a low molecular weigh chitosan. *Biomacromolecules, 8*, 322–326.

Khabashesku, V. N., Zimmerman, J. L., & Margrave, J. L. (2000). Powder synthesis and characterization of amorphous carbon nitride. *Chemistry of Materials, 12*, 3264–3270.

Kim, J., Yun, S., & Ounaies, Z. (2006). Discovery of cellulose as a smart material. *Macromolecules, 39*, 4202–4206.

Liu, J., Rinzler, A. G., Dai, H., Hafner, J., Bradley, R., Lu, A., et al. (1998). Fullerene pipes. *Science, 280*, 1253–1256.

Lu, F. S., Gu, L. R., Meziani, M. J., Wang, X., Luo, P. G., Veca, L. M., et al. (2009). Advances in bioapplications of carbon nanotubes. *Advanced Material, 21*, 139–152.

Martins, M. C. L., Wang, D., Ji, J., Feng, L., & Barbosa, M. A. (2003). Albumin and brinogen adsorption on Cibacron blue F3G-A immobilised onto PU-PHEMA (polyurethane-poly(hydroxylethyl meth-acrylate)) surfaces. *Journal of Biomaterials Science. Polymer Edition, 14*, 439–455.

Masllorens, J., Roglans, A., Moreno-Mañas, M., & Parella, T. (2004). Novel homo- and heterobimetallic palladium(0) and platinum(0) complexes of olefinic mono-, bis-, and tris-macrocyclic ligands. *Organometallics, 23*, 2533–2540.

Niesz, K., Siska, A., Vesselényi, I., Hernadi, K., Méhn, D., Galbács, G., et al. (2002). Mechanical and chemical breaking of multiwalled carbon nanotubes. *Catalysis Today, 76*, 3–10.

Ning, Y. C. (2000). *Structural identification of organic compounds and organic spectroscopy*. Beijing: Science Press.

Peng, H. Q., Alemany, L. B., Margrave, J. L., & Khabashesku, V. N. (2003). Sidewall carboxylic acid functionalization of single-walled carbon nanotubes. *Journal of the American Chemical Society, 125*, 15174–15182.

Ramanathan, T., Fisher, F. T., Ruoff, R. S., & Brinson, L. C. (2005). Amino-functionalized carbon nanotubes for binding to polymers and biological systems. *Chemistry of Materials, 17*, 1290–1295.

Romero, R. B., Leite, C. A. P., & Goncalves, M. C. (2009). The effect of the solvent on the morphology of cellulose acetate/montmorillonite nanocomposites. *Polymer, 50*, 161–170.

Saito, T., Matsushige, K., & Tanaka, K. (2002). Chemical treatment and modification of multi-walled carbon nanombes. *Physica B: Physics of Condensed Matter, 323*, 280–283.

Salmain, M., Fischer-Durand, N., Roche, C., & Pradier, C. M. (2006). Immobilization of atrazine on gold, a first step towards the elaboration of an indirect immunosensor: Characterization by XPS and PM-IRRAS. *Surface Interface Analysis, 38*, 1276–1284.

Vollhardt, D., Liu, F., & Rudert, R. (2005). The role of nonsurface-active species at interfacial molecular recognition by melamine-type monolayers. *Journal of Physical Chemistry B, 109*, 17635–17643.

Wada, S., Murata, Y., Tokunaga, A. T., & Watanabe, J. (2003). Experimental study of amorphous silicate formation. *Astronomy & Astrophysics, 406*, 783–788.

Wagner, C. D., Naumkin, A. V., Kraut-Vass, A., Allison, J. W., Powell, C. J., & Rumble, J. R., Jr. (2007). *NIST X-ray photoelectron spectroscopy database, Version 3.5 (Web Version)*. National Institute of Standards and Technology.

Xing, Q. Y., Xu, R. Q., Zhou, Z., & Pei, W. W. (2000). *Basic organic chemistry*. Beijing: Advanced Education Press.

Yang, Y. K., Xie, X. L., Yang, Z. F., Wang, X. T., Cui, W., Yang, J. Y., et al. (2007). Controlled synthesis and novel solution rheology of hyperbranched poly(urea-urethane)-functionalized multiwalled carbon nanotubes. *Macromolecules, 40*, 5858–5867.

Yu, M., Funke, H. H., Falconer, J. L., & Noble, R. D. (2009). High density, vertically-aligned carbon nanotube membranes. *Nano Letters, 9*, 225–229.

Zhang, W., Nowlan, D. T., III, Thomson, L. M., Lackowski, W. M., & Simanek, E. E. (2001). Orthogonal, convergent syntheses of dendrimers based on melamine with one or two unique surface sites for manipulation. *Journal of the American Chemical Society, 123*, 8914–8922.

Zhang, L. P., & Wang, P. W. (1995). Effect of chloride on the structure of fluoroaluminate glasses studied by XPS. *Journal of the American Ceramic Society, 78*, 2401–2404.